Hydrogen Exchange in a Bacterial Cytochrome *c*: A Fingerprint of the Cytochrome *c* Fold†

Ilaria Bartalesi,‡,§ Antonio Rosato,*,‡,§ and Wei Zhang||

Magnetic Resonance Center, University of Florence, Via Luigi Sacconi 6, 50019, Sesto Fiorentino, Italy, Department of Chemistry, University of Florence, Via della Lastruccia 3, 50019, Sesto Fiorentino, Italy, and Institute of Life Sciences and Chemistry, Roskilde University, P.O. Box 260, DK-4000, Roskilde, Denmark

Received May 19, 2003; Revised Manuscript Received July 14, 2003

ABSTRACT: The hydrogen exchange rates of backbone amides in a minimal (71 amino acid long) monoheme cytochrome *c* were determined as a function of pH in the absence and in the presence of guanidinium chloride. These data permitted the identification of units undergoing the opening reaction that precedes hydrogen exchange through a common mechanism. The opening units broadly correlate with the secondary structure elements of the protein. It is found that, despite the significant difference in primary sequence, the distribution of the opening units within the three-dimensional structure of the cytochrome studied here closely resembles that determined in mitochondrial *c*-type cytochromes. It is proposed that the observed distribution represents a fingerprint of the cytochrome *c* fold and has a role in directing the folding/unfolding of the protein.

c-type cytochromes bind one or more heme cofactors through the formation of a covalent thioether bond to the side chains of two cysteines per heme moiety. Given their vast diffusion throughout all kingdoms of life, their involvement in key biological processes (e.g., respiration in eukaryotes), and their relative ease of purification, *c*-type cytochromes have been the subject of a huge body of literature. In the last years, several studies have focused on the details of their folding/unfolding properties, so that *c*-type cytochromes have become a paradigm for metalloprotein folding/unfolding studies. Most of the work in the field has been performed on monoheme mitochondrial (usually yeast, horse heart, or tuna) proteins, which are very similar in sequence to one another (*1*, *2*). Bacterial *c*-type cytochromes, on the other hand, are widely divergent in sequence, even when only those with His/Met axial coordination are taken into account (*1*, *3*). In addition, while mitochondrial *c*-type cytochromes are all about 100−110 residue long, bacterial cytochromes can be much shorter. As an example, the soluble domain of membrane-anchored *Bacillus pasteurii* cytochrome c_{553} is only 70 residue long (*4*), which makes it one of the monoheme cytochromes with the highest heme to number of amino acids ratio (*5*). Even though mitochondrial and bacterial *c*-type cytochromes display some fundamental differences, they all share, besides the signature for covalent heme attachment, a number of basic features characterizing the cytochrome *c* fold, which had been identified in a seminal work by Chothia and Lesk (*6*).

Given the observations summarized in the preceding paragraph, the question arises as to how the folding/unfolding properties of mitochondrial and bacterial *c*-type cytochromes are related, e.g., with respect to the presence and distribution of local opening units and of the corresponding free energies of opening events. Indeed, owing to the significant differences in sequence and in size, the variation of chemical and physical properties between these two broad groups of cytochromes can be extremely large (*1*, *3*). Just to give an example, which is linked to folding/unfolding properties, it is known that the methionine axially bound to the iron ion under native conditions can be displaced by the side chain of an alternative amino acid acting as ligand or by a water molecule, depending on the environment to which the protein is exposed. This occurs most easily in the oxidized [iron(III)] state. The conditions needed to induce misligation can vary dramatically in different *c*-type cytochromes, so that the axial methionine can detach from the iron(III) ion at room temperature and neutral pH in the absence of denaturant in some systems (*7*, *8*), at alkaline pH (*9*, *10*), or in the presence of a low concentration of denaturants (*11*, *12*) in others, or may even require nearly complete unfolding of the polypeptide chain in some other proteins (*13*). A model of the alkaline form of yeast cytochrome *c* that recently became available indicates that in this system detachment of the axial methionine is accompanied by structural rearrangements mostly limited to the methionine loop (*14*). Detailed data on the folding and unfolding mechanisms of bacterial cytochromes *c* are needed to complement the information available for the more homogeneous mitochondrial proteins. This will permit the separation of individual, sequence-specific characteristics of the folding/unfolding processes and

† Financial support by MIUR and by the EC (Contract HPRI-CT-2001-00147) is gratefully acknowledged.

* Address correspondence to this author at the Magnetic Resonance Center, University of Florence. Tel: +39 055 4574267. Fax: +39 055 4574253. E-mail: rosato@cerm.unifi.it.

‡ Magnetic Resonance Center, University of Florence.

§ Department of Chemistry, University of Florence.

|| Institute of Life Sciences and Chemistry, Roskilde University.

10.1021/bi0348258 CCC: $25.00
Published on Web 08/27/2003

the identification of general trends that may constitute a fingerprint of the cytochrome *c* fold.

In this study, we have probed by NMR[1] spectroscopy the hydrogen exchange behavior of oxidized *B. pasteurii* cytochrome *c*, a minimal 71 amino acid monoheme cytochrome. pH-dependent studies have been carried out under native conditions and in the presence of 1.5 M GdmCl, where the protein is still folded (*13*). The present data permitted the identification of units exhibiting cooperative opening (termed opening units). The comparison of the structural distribution of these units with the information available for mitochondrial cytochrome *c* highlighted general "signatures" of the unfolding process of the cytochrome *c* fold, as well as protein-specific variations thereof.

MATERIALS AND METHODS

^{15}N-Enriched recombinant oxidized *Bp*cyt*c* was produced as previously reported (*15*). Note that the soluble domain used here lacks the N-terminal 21-residue membrane anchor, and thus the first amino acid of the construct is Val22 (the full-length numbering is maintained for consistency with previous works; see also ref *15*).

Hydrogen exchange experiments were performed by addition of D_2O buffer to a concentrated stock solution of ^{15}N-enriched protein to obtain samples with a final protein concentration of ca. 1 mM. A 100 mM phosphate/100 mM NH_4Cl buffer was used to buffer the pH (which was corrected for the isotope effect as described in ref *16*). All experiments were carried out at 296 K, using a 500 MHz Bruker AVANCE spectrometer equipped with a cryoprobe.

Exchange rates (k_{ex}) were determined by fitting the decay of the peak intensities in ^{1}H$-^{15}$N HSQC spectra (*17*) as a function of time to a monoexponential decay. Peak intensity decays were measured over a time range between 24 and 48 h at intervals ranging between 2 and 5 min (for the initial phase of the decay) and 30−60 min. Resonance assignments were taken from previous work (*15*).

Residue-specific free energies of exchange (ΔG_{HX}) values were obtained through application of the well-known theory of native state hydrogen exchange outlined in refs *18*−*21*. Briefly, amide hydrogen exchange is assumed to take place when the amide moiety is transiently exposed to solvent in a closed-to-open reaction:

$$\mathrm{NH(closed)} \underset{k_{cl}}{\overset{k_{op}}{\rightleftharpoons}} \mathrm{NH(open)} \xrightarrow{k_{ch}} \mathrm{exchanged} \qquad (1)$$

k_{op} is the rate at which a given amide proton is exposed to solvent, k_{cl} is the corresponding closing rate, and k_{ch} is the intrinsic exchange rate constant. In this work, k_{ch} values were estimated using the approach described by Englander and co-workers together with their parameters derived from unfolded peptide models (*22*), using Excel spreadsheets kindly provided by S. W. Englander. Under native conditions for a fully folded system the equilibrium in eq 1 is strongly shifted toward the left-hand side, and correspondingly the closing rate is generally much larger than the opening rate

[1] Abbreviations: NMR, nuclear magnetic resonance; *Bp*cyt*c*, oxidized fragment 22−92 of *Bacillus pasteurii* cytochrome c_{553}; GdmCl, guanidinium chloride; HSQC, heteronuclear single-quantum correlation spectroscopy.

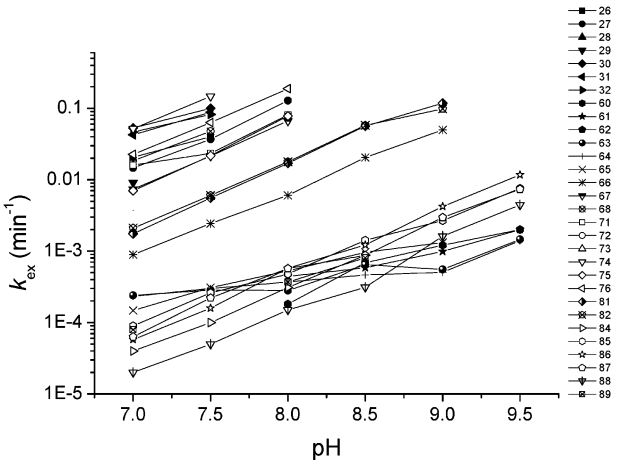

FIGURE 1: Experimental time constants for exchange (k_{ex}) plotted as a function of pH for each backbone amide moiety. Error bars are not shown for clarity; 1σ standard deviations are always smaller than twice the symbol size.

($k_{cl} \gg k_{op}$). With this assumption, the observed exchange rate (k_{ex}) of any amide group is

$$k_{ex} = k_{op}k_{ch}/(k_{cl} + k_{ch}) \qquad (2)$$

In the present system, at the lower pH values considered here the closing rate is also much faster than the intrinsic exchange rate ($k_{cl} \gg k_{ch}$, which defines the so-called "EX2 limit"), and consequently eq 2 reduces to

$$k_{ex} = K_{op}k_{ch} \qquad (3)$$

where $K_{op} = k_{op}/k_{cl}$ is the equilibrium constant for the amide opening reaction. The free energy of exchange (ΔG_{HX}) is then given by

$$\Delta G_{HX} = -RT \ln K_{op} = -RT \ln(k_{ex}/k_{ch}) \qquad (4)$$

where R is the universal gas constant and T is the temperature in kelvin. In the range of pH values used here, k_{ch} increases with increasing pH due to more efficient basic catalysis. When the pH is raised enough as to make $k_{cl} \ll k_{ch}$ ("EX1 limit"), while maintaining the system fully folded, eq 2 can be simplified to

$$k_{ex} = k_{op} \qquad (5)$$

RESULTS

Most of the amide moieties for which we could obtain reliable data at two or more different pH values are in EX2 conditions between pH 7 and pH values up to 8.5−9.0, in the absence of denaturant, as shown by the fact that the logarithm of their observed exchange rates in this range increases linearly with increasing pH, with a slope of 1.0 (Figure 1). At the lower pH values sampled here, reliable data could not be obtained for residues 60 and 61, which are part of the protein hydrophobic core, due to too slow exchange. Only upper limits can thus be estimated for these rates. At higher pH values, data for residues 60−61 were instead measurable and, together with the data relative to residues 63−65 (exchange rates for residue 62 could not be determined), indicate that the stretch 60−65 deviates from the general behavior of the remainder of the polypeptide,

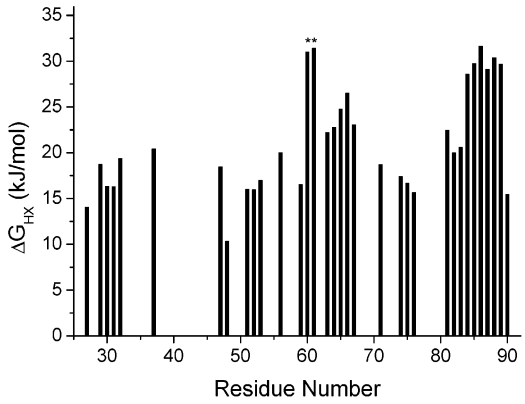

FIGURE 2: Per residue plot of the ΔG_{HX} values calculated from the backbone amide proton exchange (assumed to occur in the EX2 limit) rates measured for oxidized *B. pasteurii* cytochrome *c* in the absence of denaturant. The values for residues 60 and 61, indicated by an asterisk, are only indicative, as the exchange rates were too low to obtain a quantitative experimental estimate. Consequently, for these two residues an upper limit for the exchange rate has been used.

featuring a dependence on pH with a slope significantly lower than 1.0 (Figure 1; see also later). Note that *Bp*cyt*c* does not experience the so-called alkaline transition, featuring an axial coordination stable in the pH range 1.0−12 (*13*, *23*), which allowed us to safely perform measurements at pH values as high as 9.5. By application of eq 4, the data at pH 7.0 were used to calculate ΔG_{HX} values for oxidized *Bp*cyt*c* under native conditions (Figure 2). The exchange rates determined here do not present any significant correlation with the S^2 order parameters determined via the relaxation rates of ^{15}N nuclei of amide moieties (*15*), which is not unexpected given the fact that they depend on very different protein motions and time scales.

The values of Figure 2 are to be compared with a ΔG^{H_2O} (free energy difference between the folded and denatured protein under native conditions) obtained from protein denaturation studies of 27.2 ± 1.4 kJ mol^{-1} (*13*). The ΔG_{HX} values suggest that global opening reactions are required to bring residues in the N-terminal part of helix α_4 (residues 60−61) and in the core of helix α_5 (residues 84−89) in the exchange-competent (open) conformation under nondenaturing conditions. The two helices, α_4 and α_5, are located respectively before and after the loop containing the axial ligand to the iron, Met71. The amide moieties of the residues in the remainder of the protein instead exchange via more local conformational fluctuations. Note that some of the ΔG_{HX} values in Figure 2 are larger than ΔG^{H_2O}, which is possibly due to the fact that the free energy for global unfolding is higher in D_2O (i.e., in the present study) than in H_2O [as was the case for our previous work (*13*)] and/or to the presence of cis/trans equilibria for proline residues in the unfolded state (*24*).

In 1.5 M GdmCl the exchange rates of the amide moieties are significantly higher than in the absence of denaturant, but still in EX2 condition up to pH 8 for all the amide moieties for which reliable rates could be obtained at different pH values (not shown). Figure 3A reports the ΔG_{HX} values obtained under the conditions described in this paragraph, while the difference in ΔG_{HX} between native conditions and in the presence of 1.5 M GdmCl ($\Delta\Delta G_{HX}$) is shown on a per residue basis in Figure 3B. The data of Figure 2 indicate

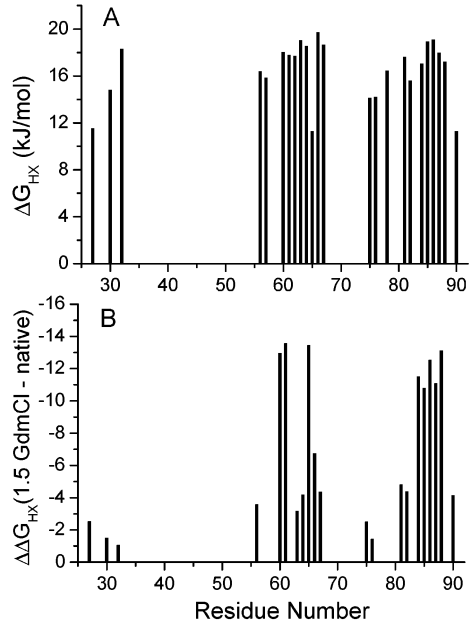

FIGURE 3: (A) Per residue plot of the ΔG_{HX} values calculated from the backbone amide proton exchange (assumed to occur in the EX2 limit) rates measured for oxidized *B. pasteurii* cytochrome *c* in the presence of 1.5 M GdmCl. (B) Per residue plot of the difference between the ΔG_{HX} values obtained in the presence and in the absence of 1.5 M GdmCl.

that there is a strong dependence of $\Delta\Delta G_{HX}$ on the presence of GdmCl for residues 63−65 and 84−88. A less pronounced dependence is observed for residues 66−67 and an even shallower dependence for the other amide moieties of the protein.

It is informative to plot k_{ex} against k_{ch}, which can be calculated to a very good approximation using available parametrizations (*22*, 25). In the EX2 regime, it is expected that this plot gives a linear relationship with a slope of 1 (*19*). Residues within units opening by the same mechanism to allow exchange to take place will define lines with essentially the same intercept (which is determined by the ΔG_{op} of that unit) (*19*, *26*). On the other hand, residues exchanging through local fluctuations are not expected to follow any particular pattern. Plotting data acquired at different pH values can extend the span of k_{ch} values, thus significantly helping to identify units and to single out possible transitions between the EX2 and EX1 exchange regime (*27*, *28*). A more commonly used approach to identify cooperatively opening units is based on measuring exchange rates as a function of [GdmCl], using ranges of concentration relatively far from the concentration promoting global unfolding (*21*, *29*). These experiments provide, besides the identification of opening units present under native conditions, information on the presence of partially unfolded forms constituting intermediates along the folding and unfolding reactions, as well as quantitative values for the ΔG and *m* parameters relative to the opening of each unit (*29*−*31*). The present approach cannot provide *m* values and, in parallel, is also not capable of identifying partially unfolded forms. On the other hand, when pH values high enough can be investigated as to observe deviations from the EX2 limit to the EX1 limit, it has the advantage of making it possible to determine the kinetics of opening and closure of the units identified thanks to the known pH dependence of k_{ch} (*28*, *32*, *33*). Finally, note that hydrogen exchange experiments

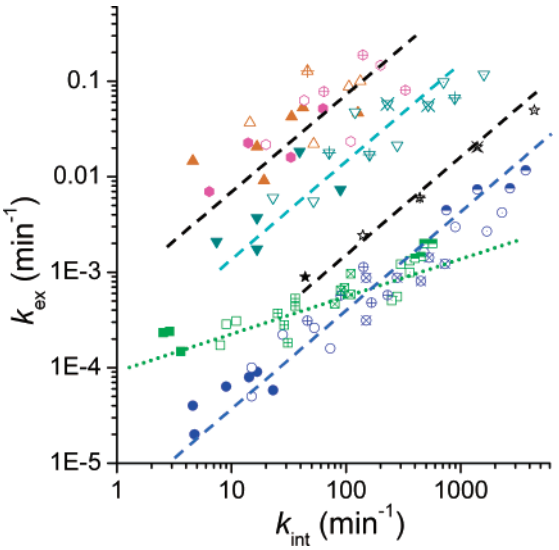

FIGURE 4: Experimental time constants for exchange (k_{ex}) at various pH values and in the absence of denaturant plotted against the corresponding calculated time constants for intrinsic exchange (k_{ch}). Key: orange up triangles, residues 26−32 and 90; green squares, residues 60−65; black stars, residue 66; dark cyan down triangles, residues 67−68 and 81−83; pink hexagons, residues 71−76; blue circles, residues 84−89; filled symbols, values at pH 7.0; open symbols, values at pH 7.5; dotted symbols, values at pH 9.0; half-filled symbols, values at pH 9.2. Lines are to guide the eye; dashed lines are parallel and have a slope of 1.0; the dotted line has a slope of 0.4.

only provide indirect evidence for the existence of units opening cooperatively and involving more than one residue (*34*, *35*). However, a close analysis of the residue-specific ΔG_{HX} values and of the distribution of residues with the same thermodynamics of exchange within the structure does permit a (tentative) identification of units exchanging via correlated motions (*35*).

Figure 4 reports the k_{ex} vs k_{ch} plot obtained on the basis of the data acquired for oxidized *Bp*cyt*c*. It is possible to identify a few different straight lines on which different groups of protein residues lie. These are shown in Figure 4, together with the corresponding dashed line with slope 1.0 (to guide the eye), and are residues 26−32, 67−68, 81−83, 66, 71−76, and 84−89. The region 60−65 appears to feature a somewhat different relationship between k_{ex} and k_{ch}, which may be indicative of deviation from the EX2 regime. Another possible cause of this behavior could be pH-dependent structural rearrangements. Figure 5 shows the distribution of the above-defined opening units onto the three-dimensional solution structure of oxidized *Bp*cyt*c*.

The data at 1.5 M GdmCl indicate an essentially linear correlation between k_{ex} and k_{ch} up to pH 7.5 (Figure S1 in the Supporting Information). Under these conditions, possibly also because of the scatter of the data, it is not possible to identify different lines for different regions of the protein, also when considering residues from regions of the protein instead belonging to different groups in the absence of denaturant.

DISCUSSION

Opening Units in Bpcytc. The present data represent an extensive characterization of equilibrium protein unfolding detected under native conditions. They complement equilibrium unfolding measurements done, e.g., by chemical denaturation, which are available for the present system (*13*), and provide information on the energetics of local opening reactions, as well as on the presence of units opening via a concerted motion within the protein structure (*29*−*31*, *36*−*38*). The system studied here is a small monoheme *c*-type cytochrome, which is structurally and functionally related to the heavily investigated mitochondrial cytochrome *c*. These two systems feature quite striking differences in terms of protein flexibility (*15*) and of fold stability (*13*). It is thus of interest to undertake detailed comparisons between the folding/unfolding properties of *Bp*cyt*c*, investigated here, and of mitochondrial cytochrome *c*, which are available from the literature.

Oxidized *Bp*cyt*c* contains five α-helices, spanning respectively residues 24−30 (α_1), 32−34 (α_2), 51−54 (α_3), 57−66 (α4), and 80−91 (α_5) (*39*) (Figure 5) (*15*). These elements of secondary structure are maintained regardless of the redox state (*40*). Figure 4 permits the identification of a few different residues with essentially the same equilibrium

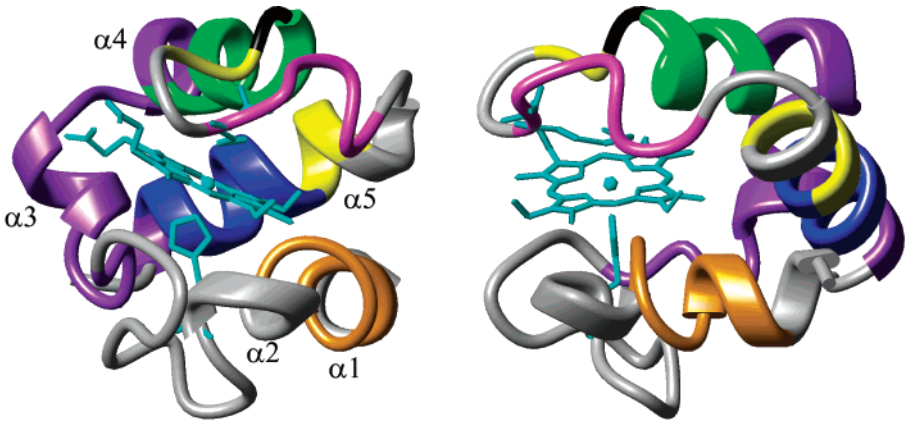

FIGURE 5: Left: Three-dimensional structure of oxidized *B. pasteurii* cytochrome *c* [PDB code 1K3H (*15*)], highlighting the different opening units identified on the basis of backbone amide proton exchange data. The heme moiety and the axial ligands are also shown (cyan). Right: Structure after rotation by 90° around the *y*-axis. Color coding is as follows: residues 26−32 are in orange; residues 60−65 are in green; residue 66 is in black; residues 67−68 and 81−83 are in yellow; residues 71−76 are in pink; residues 84−89 are in blue. Opening units displayed both in this figure and Figure 3 are shown with the same color, except for residues 67−68 and 81−83 which were dark cyan in Figure 3. All other residues for which hydrogen exchange appears to happen mainly through local fluctuations are in purple. This figure was prepared with MOLMOL (*47*).

constant for the opening reaction. The grouping of residues into different exchanging units correlates quite well with the secondary structure elements of *Bp*cyt*c*, suggesting that such units experience common opening mechanisms. The first unit along the primary sequence involves helix α_1 and the following loop (Figure 5), which could constitute the first opening unit along the primary sequence. A second unit involves residues in the loop containing the Met serving as the axial ligand to the iron ion (residues 71−76). Another unit comprises residues 67−68 and 81−83 (which are in the N-terminal part of helix α_5), which are at the boundaries of the above-mentioned loop (Figure 5). It is tempting to speculate that these residues constitute a single unit whose opening may also be linked to the opening reaction of the Met loop. Residues 60−65 (helix α_4) and 84−89 (helix α_5) constitute an additional two opening units. The latter unit has a free energy of opening which matches the free energy of global unfolding of the protein. At the lower pH values investigated, also residues 60−61, which belong to the hydrophobic core of the protein, feature high free energies of opening (indeed their exchange rates are so slow that only upper limits can be obtained) and presumably exchange through global unfolding. However, when the pH is raised at 8.0 or above, the free energies of opening of residues 60−61 drop substantially to values similar to those of residues 63−65.

For the units grouping the larger number of residues (27−32, 60−65, 71−76, and 84−89), there is relatively little spread of the residues in a particular unit around the average position of the line corresponding to each unit in Figure 4, which would suggest that strictly local opening reactions are less important in controlling the exchange reactions of individual amino acids than larger scale opening reactions such as unwinding of helical structure. Indeed, if the reverse were true, residues in the same secondary structure element would appear to be dispersed in the plots of Figure 4. This is also in agreement with the fairly small differences in ΔG_{HX} values between adjacent residues seen in Figure 2. Note that, in the unit 71−76, Met71 has the smallest equilibrium constant for opening, which may correlate with its binding to the iron ion.

The unit 60−65 displays, as already mentioned, a pH-dependent behavior, in that residues 60 and 61 join the rest of the unit only at pH values of 8 or higher (Figure 4). With raising pH, which in the range used here results in increasing k_{ch} in Figure 4 (*22*, *41*), this unit displays a correlation between k_{ex} and k_{ch}, which can be fitted to a line with a slope significantly smaller than 1. These data suggest two possible scenarios: (i) residues 60−65 are not exchanging in the EX2 regime, actually being close to the EX1 limit; (ii) structural rearrangements take place in the region 60−65 upon increasing pH. From TOCSY spectra acquired at different pH values between 7.0 and 9.0 it is not possible to detect important chemical shift variations for either backbone or side chain protons; HSQC spectra under the same conditions also do not display strong backbone nitrogen chemical shift changes. In addition, it is to be taken into account that at alkaline pH the Met−iron(III) bond is weakened, which should destabilize the native folded conformation of *Bp*cyt*c*. This would lead to enhanced amide exchange, which means a slope larger than 1.0. These considerations indicate that scenario ii above is less likely than scenario i; however, it is not possible to formulate a conclusive statement based on the present data.

Residue 66, which is the C-terminal residue of helix α_4, displays a behavior very different from that of the core part of the helix, indicating that at this end of the helix local motions start playing an important role. The following residues 67 and 68, which may form a single unit together with residues 81−83, are again behaving differently from residue 66, with a somewhat higher K_{op}. An analogous variation of the influence of local motions on the exchange process is observed for the long helix α_5 (Figure 5) where the N-terminal (81−83) and the C-terminal (residue 90) regions undergo opening more readily than the core of the helix. The higher dispersion of points in Figure 4 for the exchanging unit grouping residues 67−68 and 81−83 with respect to unit 84−89 also points to local motions being more important for the exchange process.

A close inspection of the points of Figure 4 for the two units, 66 and 67−68/81−83, reveals that at the highest pH (that is, k_{ch}) values they experience deviations from the EX2 limit. Even though they are far from reaching the EX1 limit (where one could easily obtain the value of k_{op}), fittings of the data of Figure 4 to eq 2 can provide at least an order of magnitude for k_{op} and k_{cl} for these units. The two units have the same (within error) opening rates (ca. 2.5×10^{-3} s^{-1}) and highly different closing rates (ca. 160 and 12 s^{-1}, respectively). These data may suggest a progression for local folding, whereby residue 66 is required to reach the closed state prior to closure of the unit 67−68/81−83. An analogous fitting of the data for the 60−65 region yields k_{op} ca. 1.3×10^{-5} s^{-1} and k_{cl} ca. 0.17 s^{-1}, indicative of a kinetics completely different from that of the following loop and thus, possibly, of a substantial independence in the folding/unfolding reaction.

When 1.5 M GdmCl is added to the system, a concentration which is well below the concentration required to promote global protein unfolding and detachment of the axial iron ligand (Met71) (*13*), the ΔG_{HX} values calculated from the exchange rates (Figure 3A) become close to the ΔG for global unfolding (16.8 kJ·mol^{-1}) extrapolated from the known (*13*) values of ΔG^{H_2O} (27.2 kJ·mol^{-1}) and m (6.9 kJ·M^{-1}·mol^{-1}). In addition, no individual opening units can be identified from the exchange rates measured in the presence of 1.5 M GdmCl. The above data strongly suggest that even though global unfolding of oxidized *Bp*cyt*c* at pH 7.0 occurs only at 4.1 M GdmCl (*13*), the presence of 1.5 M GdmCl is sufficient to make global exchange at least as important as local and segmental opening processes for backbone amide exchange. It is interesting to note that heteronuclear (^{15}N) relaxation measurements performed in 1.5 M GdmCl, at pH 7.0 did not reveal major changes in the dynamics of the protein backbone, while the onset of large-scale conformational exchange processes was detected only in the presence of 3.75 M GdmCl (*13*). These processes were found to affect the large majority of the polypeptide chain (*13*), which can substantiate the idea that both amide proton exchange at 1.5 GdmCl and heteronuclear relaxation measurements at 3.75 M GdmCl are sampling the global unfolding process. The different threshold for detection by the two approaches is possibly due to the very low population of the globally unfolded state at 1.5 M GdmCl (its molar fraction being around 10^{-3}, on the basis of the above estimate

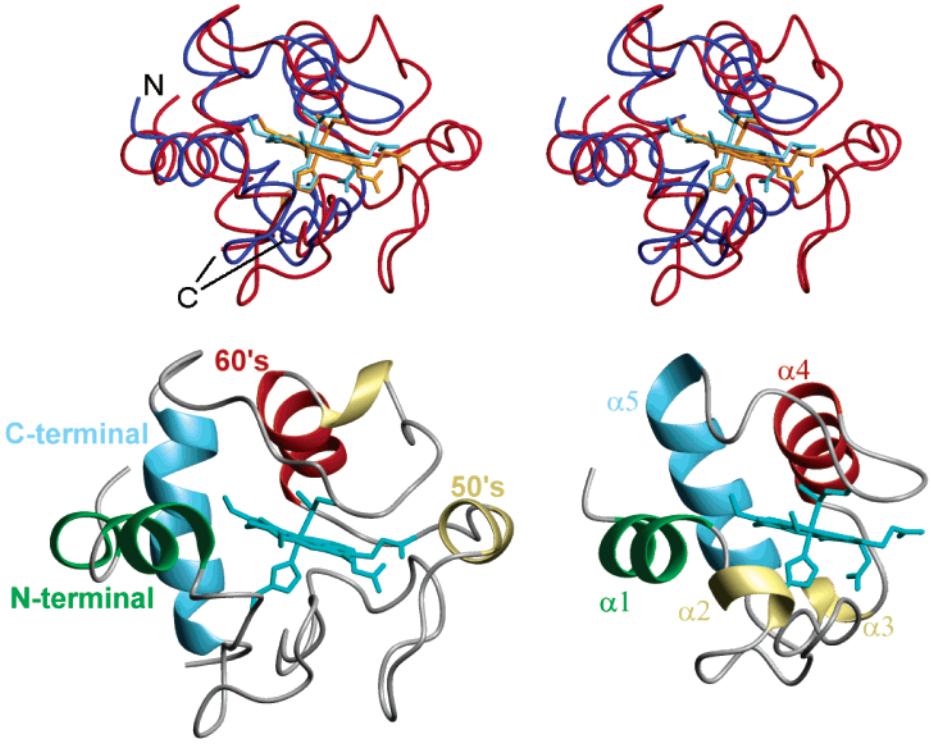

FIGURE 6: Comparison of the solution structures of oxidized mitochondrial (from horse heart) [PDB code 1AKK (*48*)] and *B. pasteurii* cytochrome *c* [DB code 1K3H (*15*)]. Top: Superposition of the structures (stereoview) based on structural alignment. *B. pasteurii* cytochrome *c* is in blue with the heme moiety and iron axial ligands in cyan; horse heart cytochrome *c* is in red with the heme moiety and iron axial ligands in orange. Bottom: Ribbon representation of the two structures (right, *B. pasteurii* cytochrome *c*; left, horse heart cytochrome *c*). Equivalent secondary structure elements have the same color, while nonequivalent structural elements are in yellow. Regions without secondary structure are in gray. The three helices homologous in the two proteins are as follows: the N-terminal helix in horse heart and α_1 in *B. pasteurii* cytochrome *c* (green); the 60's helix in horse heart and α_4 in *B. pasteurii* cytochrome *c* (red); the C-terminal helix in horse heart and α_5 in *B. pasteurii* cytochrome *c* (sky blue). This figure was prepared with MOLMOL (*47*). The structure alignment was done with the program CE (*49*). A primary sequence comparison based on the structural alignment is given in the Supporting Information.

of the free energy of unfolding). This strong difference in the relative populations of the native and unfolded state would in fact nullify the contribution of the latter to the measured ^{15}N relaxation rates. At 3.75 M GdmCl the relative population of the native and unfolded state is instead close to 1:1, which is the best condition for the detection of conformational exchange processes through ^{15}N relaxation rate measurements (*42*).

Comparison with Mitochondrial Cytochrome c. In the case of oxidized mitochondrial cytochrome *c*, it has been shown that residues in the N-terminal helix undergo opening mainly through local fluctuations, while residues in the core of the C-terminal helix can access the open state only by means of global unfolding (*29*, *38*, *43*). Local fluctuations instead do play a role for the two peripheral portions of the C-terminal helix. Residues in the other sizable helix of mitochondrial cytochrome *c*, the so-called 60's helix, exchange mainly through local fluctuations, but segmental unfolding does play a contribution (*29*). Folding of the C-terminal and N-terminal helices has been shown to happen cooperatively at the beginning of the folding pathway (*37*). Note that this is not in conflict with the fact that under native conditions the N-terminal helix exchanges more readily than the C-terminal helix through local fluctuations.

The three elements of secondary structure of mitochondrial cytochrome *c* mentioned above correspond to helices α_1, α_4, and α_5 in *Bp*cyt*c* (Figure 6 and Supporting Information). As discussed, exchange data indicate that in *Bp*cyt*c* the core regions of the α_1 and α_4 helices (respectively green and red in Figure 6) correspond to two different exchanging units, analogously to the case of the mitochondrial cytochrome *c*. Another unit is formed by the loop containing the axial Met ligand, which, again, is also observed for mitochondrial cytochrome *c*. The behavior of the exchanging unit defined by the core of helix α_5 is also very similar in the two systems, although after superposition of the heme moieties for the two proteins, this helix displays a significant difference in orientation with respect to the cofactor (sky blue helix in Figure 6). In both systems, in fact, the core of helix α_5 opens by the global exchange reaction, whereas residues at the periphery of the helix exchange through local fluctuations. Indeed, in the present system, at variance with mitochondrial cytochrome *c*, the role of segmental unwinding is more important than that of local fluctuations for the opening and exchange reactions. This is also in agreement with the fact that differences in ΔG_{HX} values between adjacent residues are smaller in the present system by, on average, a factor of 2 or more (not taking into account individual residues in mitochondrial cytochrome *c* with ΔG_{HX} values exceptionally larger with respect to neighboring residues). Notably, *Bp*cyt*c* is somewhat more rigid than mitochondrial cytochrome *c* on the submillisecond time scale (*15*), which could correlate with the less prominent role of local fluctuations.

Hydrogen exchange rates have been recently determined under native conditions for another bacterial ferricytochrome *c*, that is, cytochrome c_{551} from *Pseudomonas aeruginosa* (*44*). Also in this system, residues in the last two helices, corresponding to α_4 and α_5 of *Bp*cyt*c*, are the most protected.

A larger dispersion of protection factors than in the present case is observed. Notably, the C-terminal helix of *P. aeruginosa* has been shown to make nativelike contacts with the N-terminal helix in the transition state for protein unfolding (*45*).

Another notable difference between mitochondrial and the present cytochrome *c* is that, in the presence of 1.5 M GdmCl, the opening processes of the exchanging units of *Bp*cyt*c* discussed in the preceding paragraph may be governed by the global unfolding reaction, while in mitochondrial cytochrome *c* under these conditions the global unfolding dominates exchange for the N- and C-terminal helices but not for the 60's helix (*29*). A possible explanation could be that, because of the smaller size of the present with respect to the mitochondrial cytochrome *c*, the global unfolding reaction is comparatively more efficient in making amide protons accessible to the solvent after breakage of their H-bonding pattern (*43*). Because of the behavior of *Bp*cyt*c*, it is not possible to assess directly whether the N- and C-terminal helices constitute a single cooperative unit on the folding/unfolding pathway, as in the case of mitochondrial cytochrome *c*. However, the close resemblance of the pattern of opening reactions in the two systems strongly suggests that is the case.

CONCLUSIONS

The comparison between the opening processes underlying exchange reactions in oxidized *Bp*cyt*c* and mitochrondrial cytochrome *c* indicates that a broad similarity between the two systems exists, in that equivalent opening units can be identified. Given that the sequence identity between the two proteins is only about 22% (which reduces to 17% if the heme-binding cysteines and the iron axial ligands are not considered in the alignment), this result may suggest that the organization of opening units may be an intrinsic characteristic (a fingerprint) of the cytochrome *c* fold.

Notwithstanding the different contributions of local and segmental unwinding in different protein regions, markers of global unfolding are located in the same structural element, i.e., the C-terminal helix, despite its different packing against the heme cofactor as well as the remainder of the structure in the two proteins. This observation suggests that the high stability of the C-terminal helix may represent a requirement for the stability of the cytochrome *c* fold itself and/or that it could be instrumental in guiding the folding process of the protein (*37*, *46*). This is also in agreement with observations reported for the unrelated cytochrome c_{551} from *P. aeruginosa* (*44*, *45*).

Finally, the observation that the folding properties of oxidized *Bp*cyt*c* and mitochrondrial cytochrome *c* follow the same broad scheme reinforces the proposition that the profound difference between the stability of corresponding loops containing the axial Met ligand to the iron ion depends mostly on the structural features of the loops themselves (i.e., their packing against the other structural elements), as previously proposed (*13*).

ACKNOWLEDGMENT

We thank Prof. Ivano Bertini for careful reading of the manuscript and several useful comments.

SUPPORTING INFORMATION AVAILABLE

A figure with experimental time constants for exchange (k_{ex}) at various pH values in 1.5 M GdmCl plotted against the corresponding calculated time constants for intrinsic exchange (k_{ch}) and a figure showing a sequence comparison of *B. pasteurii* and horse heart cytochrome *c* based on their structural alignment. This material is available free of charge via the Internet at http://pubs.acs.org.

REFERENCES

1. Scott, R. A., and Mauk, A. G. (1996) in *Cytochrome c. A multidisciplinary approach*, University Science Books, Sausalito, CA.
2. Banci, L., Bertini, I., Rosato, A., and Varani, G. (1999) Mitochondrial cytochromes *c*: a comparative analysis, *J. Biol. Inorg. Chem. 4*, 824−837.
3. Ambler, R. P. (1991) Sequence variability in bacterial cytochromes, *Biochim. Biophys. Acta 1058*, 42−47.
4. Vanderberghe, I. H., Ciurli, S., Benini, S., and Van Beeumen, J. (1999) Cytochrome *c*-553 from the alkalophilic bacterium *Bacillus pasteurii* has the primary structure characteristics of a lipoprotein, *Biochem. Biophys. Res. Commun. 264*, 380−387.
5. Barker, P. D., and Ferguson, S. J. (1999) Still a puzzle: why is haem covalently attached in c-type cytochromes?, *Struct. Folding Des. 7*, R281−R290.
6. Chothia, C., and Lesk, A. M. (1985) Helix movements and the reconstruction of the haem pocket during the evolution of the cytochrome *c* family, *J. Mol. Biol. 182*, 151−158.
7. Moura, I., Liu, M. Y., Costa, C., Liu, M. C., Pai, G., Xavier, A. V., LeGall, J., Payne, W. J., and Moura, J. J. (1988) Spectroscopic characterization of a high-potential monohaem cytochrome from *Wolinella succinogenes*, a nitrate-respiring organism. Redox and spin equilibria studies, *Eur. J. Biochem. 177*, 673−682.
8. Bartalesi, I., Bertini, I., Hajieva, P., Rosato, A., and Vasos, P. (2002) Solution structure of a mono-heme ferrocytochrome *c* from *Shewanella putrefaciens* and structural analysis of sequence-similar proteins: functional implications, *Biochemistry 41*, 5112−5119.
9. Hong, X., and Dixon, D. W. (1989) NMR study of the alkaline isomerization of ferricytochrome *c*, *FEBS Lett. 246*, 105−108.
10. Pearce, L. L., Gärtner, A. L., Smith, M., and Mauk, A. G. (1989) Mutation induced perturbation of the cytochrome *c* alkaline transition, *Biochemistry 28*, 3152−3156.
11. Muthukrishnan, K., and Nall, B. T. (1991) Effective concentrations of amino acid side chains in an unfolded protein, *Biochemistry 30*, 4706−4710.
12. Russell, B. S., Melenkivitz, R., and Bren, K. L. (2000) NMR investigation of ferricytochrome *c* unfolding: detection of an equilibrium unfolding intermediate and residual structure in the denatured state, *Proc. Natl. Acad. Sci. U.S.A. 97*, 8312−8317.
13. Bartalesi, I., Bertini, I., Ghosh, K., Rosato, A., and Turano, P. (2002) The unfolding of oxidized *c*-type cytochromes: the instructive case of *B. pasteurii*, *J. Mol. Biol. 321*, 693−701.
14. Assfalg, M., Bertini, I., Dolfi, A., Turano, P., Mauk, A. G., Rosell, F. I., and Gray, H. B. (2003) Structural model for an alkaline form of ferricytohrome *c*, *J. Am. Chem. Soc. 125*, 2913−2922.
15. Banci, L., Bertini, I., Ciurli, S., Dikiy, A., Dittmer, J., Rosato, A., Sciara, G., and Thompsett, A. (2002) NMR solution structure, backbone mobility and homology modeling of *c*-type cytochromes from gram-positive bacteria, *Chem. Biol. Chem. 3*, 299−310.
16. Glasoe, P. K., and Long, F. A. (1960) Use of glass electrodes to measure acidities in deuterium oxide, *J. Phys. Chem. 64*, 188−190.
17. Bodenhausen, G., and Ruben, D. J. (1980) Natural abundance nitrogen-15 NMR by enhanced heteronuclear spectroscopy, *Chem. Phys. Lett. 69*, 185−188.
18. Berger, A., and Linderstrøm-Lang, K. (1957) Deuterium exchange of poly-D,L-alanine in aqueous solution, *Arch. Biochem. Biophys. 69*, 106−118.
19. Hvidt, A., and Nielsen, S. O. (1966) Hydrogen exchange in proteins, *Adv. Protein Chem. 21*, 287−386.
20. Englander, S. W., and Kallenbach, N. R. (1983) Hydrogen exchange and structural dynamics of proteins and nucleic acids, *Q. Rev. Biophys. 16*, 521−655.

21. Huyghues-Despointes, B. M., Pace, C. N., Englander, S. W., and Scholtz, J. M. (2001) Measuring the conformational stability of a protein by hydrogen exchange, *Methods Mol. Biol. 168*, 69−92.
22. Bai, Y., Milne, J. S., Mayne, L., and Englander, S. W. (1993) Primary structure effects on peptide group hydrogen exchange, *Proteins: Struct., Funct., Genet. 17*, 75−86.
23. Benini, S., Borsari, M., Ciurli, S., Dikiy, A., and Lamborghini, M. (1998) Modulation of *Bacillus pasteurii* cytochrome c_{553} reduction potential by structural and solution parameters, *J. Biol. Inorg. Chem. 3*, 371−382.
24. Bai, Y., Milne, J. S., Mayne, L., and Englander, S. W. (1994) Protein stability parameters measured by hydrogen exchange, *Proteins: Struct., Funct., Genet. 20*, 4−14.
25. Connelly, G. P., Bai, Y., Jeng, M. F., and Englander, S. W. (1993) Isotope effects in peptide group hydrogen exchange, *Proteins: Struct., Funct., Genet. 17*, 87−92.
26. Yan, S., Kennedy, S. D., and Koide, S. (2002) Thermodynamic and Kinetic Exploration of the Energy Landscape of Borrelia burgdorferi OspA by Native-state Hydrogen Exchange, *J. Mol. Biol. 323*, 363−375.
27. Robertson, A. D., and Murphy, K. P. (1997) Protein structure and the energetics of protein stability, *Chem. Rev. 97*, 1251−1267.
28. Kalodimos, C. G., Boelens, R., and Kaptein, R. (2002) A residue-specific view of the association and dissociation pathway in protein−DNA recognition, *Nat. Struct. Biol. 9*, 193−197.
29. Bai, Y. W., Sosnick, T. R., Mayne, L., and Englander, S. W. (1995) Protein folding intermediates: native-state hydrogen exchange, *Science 269*, 192−197.
30. Chu, R., Pei, W., Takei, J., and Bai, Y. (2002) Relationship between the native-state hydrogen exchange and folding pathways of a four-helix bundle protein, *Biochemistry 41*, 7998−8003.
31. Takei, J., Pei, W., Vu, D., and Bai, Y. (2002) Populating partially unfolded forms by hydrogen exchange-directed protein engineering, *Biochemistry 41*, 12308−12312.
32. Arrington, C. B., and Robertson, A. D. (1997) Microsecond protein folding kinetics from native-state hydrogen exchange, *Biochemistry 36*, 8686−8691.
33. Sivaraman, T., Arrington, C. B., and Robertson, A. D. (2001) Kinetics of unfolding and folding from amide hydrogen exchange in native ubiquitin, *Nat. Struct. Biol. 8*, 331−333.
34. Arrington, C. B., Teesch, L. M., and Robertson, A. D. (1999) Defining protein ensembles with native-state NH exchange: kinetics of interconversion and cooperative units from combined NMR and MS analysis, *J. Mol. Biol. 285*, 1265−1275.
35. Arrington, C. B., and Robertson, A. D. (2000) Correlated motions in native proteins from MS analysis of NH exchange: evidence for a manifold of unfolding reactions in ovomucoid third domain, *J. Mol. Biol. 300*, 221−232.
36. Sauder, J. M., and Roder, H. (1998) Amide protection in an early folding intermediate of cytochrome *c*, *Folding Des. 3*, 293−301.
37. Hoang, L., Bedard, S., Krishna, M. M., Lin, Y., and Englander, S. W. (2002) Cytochrome *c* folding pathway: kinetic native-state hydrogen exchange, *Proc. Natl. Acad. Sci. U.S.A. 99*, 12173−12178.
38. Maity, H., Lim, W. K., Rumbley, J. N., and Englander, S. W. (2003) Protein hydrogen exchange mechanism: Local fluctuations, *Protein Sci. 12*, 153−160.
39. Benini, S., Rypniewski, W., Wilson, K. S., Van Beeumen, J., and Ciurli, S. (2000) Crystal structure of oxidized *Bacillus pasteurii* cytochrome c_{553} at 0.97 Å resolution, *Biochemistry 39*, 13115−13126.
40. Bartalesi, I., Bertini, I., and Rosato, A. (2003) Structure and dynamics of reduced *Bacillus pasteurii* cytochrome *c*: oxidation state dependent properties and implications for electron-transfer processes, *Biochemistry 42*, 739−745.
41. Wüthrich, K. (1986) in *NMR of Proteins and Nucleic Acids*, Wiley, New York.
42. Luz, Z., and Meiboom, S. (1963) Nuclear magnetic resonance study of the protolysis of trimethylamminium ion in aqueous solution-order of the reaction with respect to solvent., *J. Chem. Phys. 39*, 370.
43. Milne, J. S., Mayne, L., Roder, H., Wand, A. J., and Englander, S. W. (1998) Determinants of protein hydrogen exchange studied in equine cytochrome *c*, *Protein Sci. 7*, 739−745.
44. Russell, B. S., Zhong, L., Bigotti, M. G., Cutruzzolà, F., and Bren, K. L. (2003) Backbone dynamics and hydrogen exchange of *Pseudomonas aeruginosa* ferricytochrome c_{551}, *J. Biol. Inorg. Chem. 8*, 156−166.
45. Gianni, S., Travaglini-Allocatelli, C., Cutruzzolà, F., Bigotti, M. G., and Brunori, M. (2001) Snapshots of protein folding. A study on the multiple transition state pathway of cytochrome *c*(551) from *Pseudomonas aeruginosa*, *J. Mol. Biol. 309*, 1177−1187.
46. Lyubovitsky, J. G., Gray, H. B., and Winkler, J. R. (2002) Mapping the cytochrome *c* folding landscape, *J. Am. Chem. Soc. 124*, 5481−5485.
47. Koradi, R., Billeter, M., and Wüthrich, K. (1996) MOLMOL: a program for display and analysis of macromolecular structure, *J. Mol. Graphics 14*, 51−55.
48. Banci, L., Bertini, I., Gray, H. B., Luchinat, C., Reddig, T., Rosato, A., and Turano, P. (1997) Solution structure of oxidized horse heart cytochrome *c*, *Biochemistry 36*, 9867−9877.
49. Shindyalov, I. N., and Bourne, P. E. (1998) Protein structure alignment by incremental combinatorial extension (CE) of the optimal path, *Protein Eng. 11*, 739−747.

BI0348258